Simultaneous Electroencephalographic and Functional Magnetic Resonance Imaging Indicate Impaired Cortical Top–Down Processing in Association with Anesthetic-induced Unconsciousness

Denis Jordan, Ph.D.,* Rüdiger Ilg, M.D.,† Valentin Riedl, Ph.D.,‡ Anna Schorer, M.D.,§ Sabine Grimberg, M.D.,‖ Susanne Neufang, Ph.D.,‡ Adem Omerovic, M.Sc.,# Sebastian Berger, M.Sc.,# Gisela Untergehrer, M.D.,** Christine Preibisch, Ph.D.,‡ Enrico Schulz, Ph.D.,†† Tibor Schuster, Ph.D.,‡‡ Manuel Schröter, Ph.D.,§§ Victor Spoormaker, Ph.D.,§§ Claus Zimmer, M.D.,‖‖ Bernhard Hemmer, M.D.,## Afra Wohlschläger, Ph.D.,‡ Eberhard F. Kochs, M.D.,*** Gerhard Schneider, M.D.†††

ABSTRACT

Background: In imaging functional connectivity (FC) analyses of the resting brain, alterations of FC during unconsciousness have been reported. These results are in accordance with recent electroencephalographic studies observing impaired top–down processing during anesthesia. In this study, simultaneous records of functional magnetic resonance imaging (fMRI) and electroencephalogram were performed to investigate the causality of neural mechanisms during propofol-induced loss of consciousness by correlating FC in fMRI and directional connectivity (DC) in electroencephalogram.

Methods: Resting-state 63-channel electroencephalogram and blood oxygen level–dependent 3-Tesla fMRI of 15 healthy subjects were simultaneously registered during consciousness and propofol-induced loss of consciousness. To indicate DC, electroencephalographic symbolic transfer entropy was applied as a nonlinear measure of mutual interdependencies

What We Already Know about This Topic

- Anesthesia-induced unconsciousness seems to involve impairment of top–down processing of information; as detected *either* by functional magnetic resonance imaging or the electroencephalographic methods

What This Article Tells Us That Is New

- Both *simultaneous* electroencephalographic and functional magnetic resonance imaging measurements confirmed a decreased connectivity in frontoparietal feedback networks with propofol-induced loss of consciousness

* Research Fellow, ‖ Resident, # Research Assistant, *** Professor, Director Chair, Department of Anesthesiology, † Associate Professor, § Resident, †† Research Fellow, ## Professor, Director Chair, Department of Neurology, ‡ Research Fellow, ‖‖ Professor, Director Chair, Department of Neuroradiology, Klinikum rechts der Isar, Technische Universität München, Munich, Germany. ‡‡ Research Fellow, Department of Medical Statistics and Epidemiology, Technische Universität München, Munich, Germany. §§ Research Fellow, Max Planck Institute of Psychiatry, Munich, Germany. ** Resident, ††† Professor, Director Chair, Department of Anesthesiology, Klinikum rechts der Isar, Technische Universität München, and Department of Anesthesiology, Witten/Herdecke University, Helios Clinic Wuppertal, Wuppertal, Germany.

Received from the Departments of Anesthesiology, Neurology, and Neuroradiology, Klinikum rechts der Isar, Technische Universität München, Munich, Germany. Submitted for publication January 28, 2013. Accepted for publication July 15, 2013. Support was provided solely from institutional and/or departmental sources. The authors declare no competing interests. The first two and last two authors contributed equally to this article. Drs. Jordan and Kochs have applied for an International patent (International Application Number: PCT/EP 2012/001794, International Filing Date: April 26, 2012; Priority Date: DE 10 2011 100 173.9 filed on May 5, 2011).

Address correspondence to Dr. Ilg: Department of Neurology, Klinikum rechts der Isar, Technische Universität München, Ismaninger Straße 22, 81675 Munich, Germany. ilg@lrz.tu-muenchen.de. This article may be accessed for personal use at no charge through the Journal Web site, www.anesthesiology.org.

 Anesthesiology 2013; 119:1031-42

◇ This article is featured in "This Month in Anesthesiology." Please see this issue of ANESTHESIOLOGY, page 1A.

◆ This article is accompanied by an Editorial View. Please see: Mashour GA: Consciousness and the 21st century operating room. ANESTHESIOLOGY 2013; 119:1003-5.

Supplemental digital content is available for this article. Direct URL citations appear in the printed text and are available in both the HTML and PDF versions of this article. Links to the digital files are provided in the HTML text of this article on the Journal's Web site (www.anesthesiology.org).

between underlying physiological processes. The relationship between FC of resting-state networks of the brain (*z* values) and DC was analyzed by a partial correlation.

Results: Independent component analyses of resting-state fMRI showed decreased FC in frontoparietal default networks during unconsciousness, whereas FC in primary sensory networks increased. DC indicated a decline in frontal–parietal (area under the receiver characteristic curve, 0.92; 95% CI, 0.68–1.00) and frontooccipital (0.82; 0.53–1.00) feedback DC ($P < 0.05$ corrected). The changes of FC in the anterior default network correlated with the changes of DC in frontal–parietal ($r_{partial} = +0.62$; $P = 0.030$) and frontal–occipital (+0.63; 0.048) electroencephalographic electrodes ($P < 0.05$ corrected).

Conclusion: The simultaneous propofol-induced suppression of frontal feedback connectivity in the electroencephalogram and of frontoparietal FC in the fMRI indicates a fundamental role of top–down processing for consciousness.

THE neural correlates of the hypnotic component of anesthesia and, in more general, unconsciousness are still poorly understood. One of the mysteries about general anesthesia is that, despite their diverse molecular structures and different receptor profiles, all anesthetics induce reversible loss of consciousness (LOC).[1–4] Theoretical models suggested an impaired capacity of the brain to integrate information across specialized subsystems as common denominator.[1,4–6] Following this reasoning, several studies have investigated the effects of general anesthesia on the functional connectivity (FC) in the resting brain and have found connectivity changes of cortical and subcortical networks.[7–10] For example, FC in the frontoparietal networks was found to be decreased during propofol-induced LOC (PI-LOC), whereas FC in the lower-order sensory cortices remained unchanged.[7] This could be interpreted in terms of decreased higher-order cognitive processing, whereas lower-order sensory processes were obviously preserved. Recent graph theoretical analyses of spontaneous blood oxygen level–dependent (BOLD) fluctuations in functional magnetic resonance imaging (fMRI) under PI-LOC demonstrated a general reconfiguration of the spatiotemporal organization of resting brain networks and indicated a general reduction in whole-brain spatiotemporal integration.[11] This disintegration was driven by a breakdown of subcorticocortical and corticocortical connectivity and profound decline in long-range connections. The relevance of frontal access to sensory information has been reinforced by an electroencephalographic study on vegetative-state patients who reported impaired frontal-to-temporal backward connectivity during an auditory mismatch negativity paradigm.[12] However, the results of the latter study have been critically discussed.[13] Current electroencephalographic studies demonstrated impaired frontal to parietal, top–down information processing during anesthesia.[14–18] This finding is supposed to be in line with changes of FC during anesthesia-induced LOC. The link between these results, however, is still missing, and the question of whether and to what extent the observed changes in functional brain network organization reflect information processing in the underlying neural networks is still open. A combined measurement of electroencephalogram and fMRI would provide a step forward in order to overcome methodological limitations of both methods, for example, possible alterations of BOLD signals caused by hypnotic drugs.[19] To fill this gap, we performed simultaneous measurements of FC and of directional connectivity (DC) using high-resolution electroencephalogram during PI-LOC. Whereas fMRI FC indicates a probabilistic network dependency that is based on hemodynamic fluctuations of the BOLD signal on a time-scale of several seconds, electroencephalographic DC reflects directed "real-time" interactions along information pathways within cortical networks on a time-scale of milliseconds.[20] To quantify DC we used symbolic transfer entropy (STEn), which distinguishes driving and responding subsystems in complex nonlinear dynamics and detects asymmetry in their mutual interaction.[21] STEn is based on symbolic signal analysis, which inherits the concept of permutation entropy (PeEn). Although PeEn distinguishes responsiveness from unresponsiveness by indicating decreased "information content" in the electroencephalogram recording during anesthesia,[22,23] STEn is assumed to specifically indicate anesthesia-induced effects on the systemic information processing of the brain.[15,16] Therefore, it combines advantages of a stringent concept to infer the direction of interactions with robustness of symbolic analysis. We tested the hypothesis that top–down decoupling of higher-order frontal processes represents a feature of anesthesia-induced unconsciousness.

Materials and Methods

Subjects and Study Design

Fifteen male subjects participated in the study (21–32 yr old, mean age 25.8 yr). The current combined electroencephalographic–fMRI data have been acquired in a previous graph theoretical study of spontaneous BOLD fluctuations in fMRI under PI-LOC.[11] The study protocol was in accordance with the Declaration of Helsinki and approved by the local ethics committee of the medical department of the Technische Universität München, Germany. All subjects were right-handed, drug-free, and had no history of neurological or psychiatric disorders. Subjects had to give written informed consent and were reimbursed for participation. The subjects were instructed to lie in a supine position with their eyes closed and not to fall asleep. A baseline 63-channel electroencephalogram (10 min) at wakefulness (AW) was performed outside of the magnetic resonance imaging (MRI) scanner and subsequently in the MRI scanner during the simultaneous resting-state fMRI measurement. In the MRI scanner, propofol was administered using a target-controlled infusion (TCI) pump (Open TCI; Space infusion system; Braun Medical, Melsungen, Germany) to obtain constant effect-site concentrations, as estimated by

the pharmacokinetic model of Marsh.[24] TCI concentrations were increased in 0.4 μg/ml steps beginning at 1.2 μg/ml until volunteers stopped responding to the verbal command "squeeze my hand" accompanied by a firm handshake (PI-LOC, corresponding to a Ramsay sedation scale of 5–6 (Ramsay *et al.*),[25] that is, sluggish or no response to tactile or auditory stimulation). TCI concentration at this point was maintained and kept stable for another 10 min to ensure equilibration of the estimated effect-site concentration. Having reached this equilibrium, simultaneous electroencephalogram and fMRI measurements were performed subsequently for about 10 min. After that, a phase of sedation at 50% of the PI-LOC concentration was recorded; however, movement artifacts prevented a reliable fMRI analysis of these data.

Electroencephalographic Acquisition and Preprocessing

For combined electroencephalographic–fMRI recordings, an interface unit (SyncBox; Brain Products, Gilching, Germany) was used to reduce timing-related errors in the fMRI artifact correction by synchronizing the clocks of the electroencephalographic amplifiers and the MRI gradients. The electroencephalogram was obtained using an MRI-compatible, 64-channel electrode cap with equidistantly arranged ring-type sintered nonmagnetic Ag/AgCl electrodes (Easycap, Herrsching, Germany) and two 32-channel, nonmagnetic, battery-operated electroencephalographic amplifiers (BrainAmp MR; Brain Products). One of the 64-channels was dedicated to registering the electrocardiogram and was placed over the chest (left anterior axillary line). Both of the signals were recorded with a 5 kHz sampling rate (BrainVision Recorder; Brain Products). The electroencephalographic signal preprocessing analyses were performed using a BrainVision Analyzer 2 (Brain Products). fMRI gradient artifacts in the electroencephalogram were averaged over a sliding window and subtracted from the electroencephalographic signals.[26] The cardioballistic artifacts caused by cardiomechanic electrode induction were removed using a template-detection method. The templates were based on the detected local maxima (R-peaks) and subtracted from the electroencephalogram using sliding windows of 21 epochs.[26] Finally, basic artifact rejection (sweeps with amplitudes exceeding 250 μV), average reference, and independent component analysis (ICA) for blind source separation of noncortical signal components were performed. Electroencephalographic analysis is based on fMRI gradient–synchronous signals recorded during AW and PI-LOC of all 15 subjects (63 effective channels, nonoverlapping artifact corrected signals of 10-s length at each six times the repetition time (1,838 ms) of fMRI sequence, zero-phase digital filtered with 0.5–30 Hz total bandwidth, 200 Hz sampling frequency, N = 2,000 amplitude samples per signal).

Electroencephalographic PeEn

Nonlinear electroencephalographic PeEn has been established to reliably separate AW from PI-LOC.[23] PeEn quantifies the regularity structure of the neighboring order of signal values in order to reflect "information content" of the signal.[22] Basically, distortions of the electroencephalogram recordings in high-static and radiofrequency electromagnetic fields of the MRI scanner may challenge reliability of the signal analysis. A key advantage of the nonparametric PeEn over parametric analysis methods is its robustness against artifacts, signal distortions, and poorly known characteristics of the underlying dynamics, which makes this approach comparatively rugged against a specific selection of embedding parameters (dimension m, time lag l).[23,27] Because of limitations in the signal quality of the present data, suitable embedding parameters of PeEn were based on previous electroencephalographic analyses: According to the signal length criterion $m! < N$ we used $m = 5$,[22,23,27] and $l = 5$ in order to provide a sufficient deployment of trajectories within the state space of f the electroencephalographic β-band during AW and PI-LOC.[28]

Electroencephalographic STEn

The STEn has been introduced by Staniek *et al.*[21] in 2008 and inherits advantages of nonparametric PeEn, which analyzes amplitude orders instead of absolute amplitude values. In contrast to PeEn, the STEn does not only reflect information in one single electroencephalographic channel but also indicates the directed mutual interaction between two electroencephalographic signals $x = \{x(1), x(2), \ldots, x(N)\}$ and $y = \{y(1), y(2), \ldots, y(N)\}$ containing N amplitude samples as generated by systems (*i.e.*, electrodes) X, Y. In particular, STEn detects strength and directionality of "information flow," which we used to quantify the DC. Therefore, STEn analyzes consecutive sequences $x_i = \{x(i), x(i+l), \ldots, x(i+(m-1)l\}$ and $y_i = \{y(i), y(i+l), \ldots, y(i+(m-1)l\}\,(i \in \{1, \ldots, N-(m-1)l\})$ with respect to embedding parameters m (dimension) and l (time lag) in the analyzed electroencephalographic signals x and y. The order of samples in every sequence according to their amplitudes is computed and defines permutations $\hat{x}_i, \hat{y}_i$ of order m. The degree of prediction $p(\hat{x}_i)$ of actual information in x (or y respectively) from past extrinsic information content in $\hat{y}_{i-\delta}$ (or $\hat{x}_{i-\delta}$ respectively) with respect to a transfer delay $\delta > 0$ is reflected by a generalized Markov property. Thereby, intrinsic prediction within one and the same signal is discarded by "subtracting" the probability $p(\hat{x}_{i-\delta})$ (or $p(\hat{y}_{i-\delta})$, respectively) that $\hat{x}_i$ can be explained by $\hat{x}_{i-\delta}$ (or $\hat{y}_i$ by $\hat{y}_{i-\delta}$, respectively). Summarizing, calculation of STEn predicting information in system X from information in system Y is related to information theoretic entropy definition given by C. E. Shannon, see equation (1).

$$\mathrm{STEn}_{Y\to X} = \sum p\left(\hat{x}_i, \hat{x}_{i-\delta}, \hat{y}_{i-\delta}\right) \cdot \log_2\left(\frac{p\left(\hat{x}_i \middle| \hat{x}_{i-\delta}, \hat{y}_{i-\delta}\right)}{p\left(\hat{x}_i \middle| \hat{x}_{i-\delta}\right)}\right) \quad (1)$$

The sum considers all triplets of permutations of order m in x, y, and $p(A|B)$ is the conditional probability that A occurs under condition B, $p(A, B)$ is the joint probability of A and B. The directionality index, here denoted by STEn, quantifies the preferred direction of flow between systems X and Y as described in equation (2).

$$\mathrm{STEn} = \mathrm{STEn}_{X\to Y} - \mathrm{STEn}_{Y\to X} \quad (2)$$

Symbolic transfer entropy is expected to attain positive values for unidirectional coupling with X as the driver and negative values for Y driving X. Assuming $\mathrm{STEn}_{X\to Y}, \mathrm{STEn}_{Y\to X} > 0$, a value STEn = 0 would indicate symmetric bidirectional coupling. A calculation example of $\mathrm{STEn}_{Y\to X}$ is shown in figure 1. In the present analysis, STEn was computed over all channel pair combinations. Similar to PeEn, STEn is less sensitive to the choice of specific embedding parameters than comparable parametric measures of directed mutual interaction.[16,21,29–31] As for PeEn we used $m = 5$, $l = 5$, and a transfer delay $\delta = 7 - 12$ corresponding to 35–60 ms. Because the STEn is computed in the time space, a direct comparison to frequency-based signal analysis is not meaningful. Nevertheless, the applied settings result in a focus on information transfer in time scales within the electroencephalographic β-band, which is suspected to be relevant for long-range intercortical information exchange.[32,33] If not specified, STEn is used below as a common shortcut for the directionality index and for $\mathrm{STEn}_{X\to Y}, \mathrm{STEn}_{Y\to X}$.

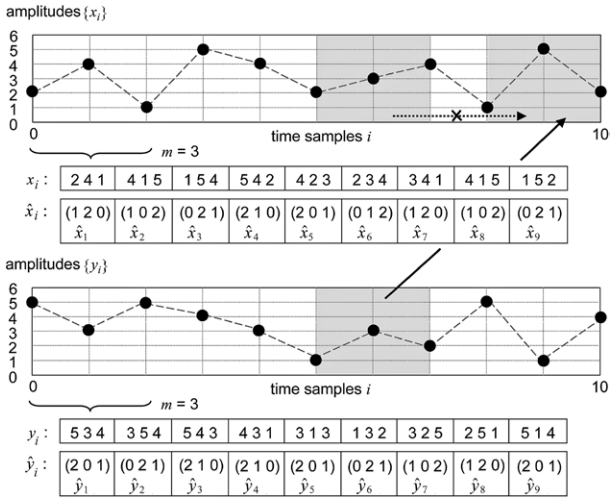

Fig. 1. Calculation scheme for symbolic transfer entropy ($\mathrm{STEn}_{Y\to X}$) reflecting transfer from system Y to X is based on exemplary electroencephalographic signals x and y (embedding dimension $m = 3$, time lag $l = 1$). First, consecutive subvectors of the length m containing amplitude values are extracted from both signals. Second, a ranking of the amplitudes for every obtained subvector is defined resulting in permutations $\hat{x}_i, \hat{y}_i$ along both signals. Third, probabilities describing how good the actual order sequence with respect to a transfer delay $\delta = 3$ can be explained extrinsically from a previous sequence (here only shown at $t = 9$: $\hat{y}_{9-\delta} = \hat{y}_6$ predicts $\hat{x}_9$ without intrinsic information of $\hat{x}_6$. $\mathrm{STEn}_{Y\to X} = 0.50$ is obtained by summation over all available permutations in x and y.

Computation of PeEn and STEn was performed using LabVIEW 8.5 (National Instruments, Austin, TX), where the core algorithms of PeEn and STEn were embedded in C, allowing parallel processing on an Intel Xeon–based workstation with Windows 7 (Microsoft Corporation, Redmond, WA).

Electroencephalographic DC Analysis

The effects of propofol on the PeEn in frontal, parietal, temporal, and occipital electroencephalogram (changes of "information content") such as on the STEn–based DC in frontal–parietal, frontal–temporal, frontal–occipital, parietal–temporal, parietal–occipital, and temporal–occipital electroencephalogram (changes of DC) were indicated. Therefore, values of PeEn and of STEn in frontal (18 electrodes corresponding to Fp1-FC6 according to the 10–20 scheme), central (11 electrodes, C5-CP4), parietal (14 electrodes, P11-PO8), temporal (12 electrodes, FT1-TP12), and occipital (8 electrodes, O9-I12) recordings on the electroencephalogram were averaged. Discrimination of PeEn and STEn between AW and PI-LOC was evaluated using the area under the receiver characteristic curve (AUC). The AUC represents a nonparametric (independent from scale units and from assumptions on underlying distributions) statistical measure quantifying the correlation between observed clinical states (*i.e.*, AW *vs.* PI-LOC) and a classifier (*i.e.*, PeEn, STEn). It allows a simple interpretation, as AUC = 1 indicates a completely concordant relation between the clinical state and the classifier, AUC = 0 implies completely discordant relation, and AUC = 0.5 means that the classifier's results are as good as a random process with two possible outcomes. To determine the uncertainty of the realization of the test statistic, 95% two-sided percentile bootstrap CIs were applied at Bonferroni-corrected threshold P value of less than 0.05 for multiple tests (PK Tool; Department of Anesthesiology, Klinikum rechts der Isar, Technische Universität München, Munich, Germany).[34,35] CI includes additional correction for multiple measurements by including only one random data point per subject and condition (AW, PI-LOC) for each bootstrap sample.[34,36] To verify that STEn provided comparable results inside and outside the MRI scanner environment, results of both recordings during AW were compared using a permutation test with T^2 statistics for multivariate data (threshold $P < 0.05$; R Foundation for Statistical Computing, Vienna, Austria).[37] Additionally, results of STEn obtained from the average reference and from referential FCz electrode montage were compared (permutation test with T^2 statistics for multivariate data). STEn may indicate spurious interdependencies in the electroencephalogram recordings caused by spectral changes. Therefore, we derived surrogates from the electroencephalographic signals: With the use of an iterative procedure of the amplitude-adjusted Fourier transform method,[38] surrogates inherit linear properties from the electroencephalogram (mean, variance, and autocovariance structure) by preserving the amplitude distribution but changing underlying dynamics to a linear random process. Differences

between STEn of the electroencephalogram and of surrogates as caused by signal nonlinearity are estimated using CI (Bonferroni-corrected threshold $P < 0.05$ based on 20 surrogates per electroencephalographic signal at AW and at PI-LOC).[16]

fMRI Acquisition and Preprocessing

The FC analyses refer to the fMRI data of the previously reported graph theoretical network analyses.[11] To study the effects of PI-LOC on the FC of brain networks, we performed an ICA of BOLD fluctuations in fMRI at rest. Therefore, a 3-Tesla whole-body MRI scanner (Achieva Quasar Dual; Philips, Amsterdam, The Netherlands) with an eight-channel, phased-array head coil was used. The rest of the data were collected using a gradient echo planar imaging sequence (echo time = 30 ms, repetition time = 1,838 ms, flip angle = 75°, field of view = 220 × 220 mm^2, matrix = 72 × 72, 32 slices, slice thickness = 3 mm, and 1-mm interslice gap; 10-min acquisition time, resulting in 300 volumes). fMRI data were preprocessed using statistical parametric mapping (SPM) 5.‡‡‡ This process consisted of realigning the images to correct for motion and related susceptibility artifacts and of spatially normalizing all the images to the standard Montreal Neurological Institute echo planar imaging template. Finally, the images were resampled to a voxel resolution of 2 × 2 × 2 mm^3 using a fifth-degree spline interpolation and smoothed with an 8-mm Gaussian kernel. Only scans with head movements less than 2 mm between two subsequent slices were accepted for further analysis. The data were corrected for slice time to account for interleaved slice acquisition. The six head movement parameters from the realignment and global signals within the white matter and ventricular cerebrospinal fluid were defined in a multiple regression model to remove unspecific signal variation from the time series.

fMRI FC Analysis

For the independent component network (ICN) analyses, the preprocessed data were decomposed into spatially independent components within a group ICN analysis (ICA) framework using the GIFT software.§§§ The dimensionality estimation was performed using the minimum description length criteria, resulting in 36 independent components that represented the mean of all the individual estimates. Before the volumes were entered into the ICA, a voxel-wise z-transformation on the time course data was performed. The calculated scaling factor was reintegrated into the data by voxel-wise multiplication before entering the individual's spatial maps into the second-level statistics to preserve each individual's variance magnitude profile while leaving the normalized time course of the component unchanged.[39] In this manner, the multivariate ICA algorithm for correlating the variance between voxels, that is, the FC, was rendered independent of the original BOLD signal magnitude across the subjects. The data were concatenated and reduced by a two-step principal component analysis, followed by an independent component estimation using the Infomax algorithm.[40] The stability of the estimated components was ensured using 30 ICASSO iterations.[41] The subject-specific components, as represented by the spatial maps with unit variance and associated time courses, were subsequently obtained using a back reconstruction algorithm. We then used SPM 5 and SPM 8 (Wellcome Trust Centre for Neuroimaging, University of London, London, United Kingdom) to perform the statistical analysis of higher cortical networks and primary sensory networks that were hypothetically affected by the anesthesia, that is, the default mode network (DMN) and primary visual and auditory networks.[7] These networks were identified on the basis of extensive previous research on resting-state networks of the brain.[42] For the statistical analysis of the connectivity changes between the conditions, we defined a 1 × 2 ANOVA model (full-factorial design) with "condition" as the within-subject factor (AW *vs.* PI-LOC) and spatial field maps resulting from ICA analysis as dependent variables. We explicitly masked the condition comparisons using the network masks that resulted from the F-contrast. As a secondary variable, to investigate the effect of thalamocortical coupling, we performed a correlation analysis of the time courses of a thalamic region of interest and cortical ICNs (two-way repeated-measures ANOVA model). The results are reported using the height threshold P value less than 0.001 (uncorrected) at the voxel level and extent threshold P value less than 0.05 (family-wise error corrected) at the cluster level.

Correlation Analysis of FC (fMRI) and DC (Electroencephalogram)

Addressing the hypothesis of propofol-induced changes of higher-order frontal processes, the relationship between FC and direction of interaction (DC) in individuals was investigated by removing the differences between subjects and looking at the changes within. Therefore, we performed a partial correlation analysis (with the corresponding t test for the regression slope) between the individual mean z scores of frontoparietal ICNs and mean STEn ($r_{partial}$) at a threshold P value of less than 0.05.[43,44] Partial correlation considers repeated observations (both conditions AW and PI-LOC) and takes into account the variability of measurements made on different subjects and the variability between measurements. Variations due to the subject-related factors were removed by ANOVA.

Results

Propofol Concentration and Cardiorespiratory Monitoring

Propofol-induced LOC (denoted as individuals having a loss of response to repeated verbal commands) occurred at mean TCI effect-site plasma concentration of 2.97 μg/ml (SD, 0.47 μg/ml). During PI-LOC, the subjects showed a statistically significant drop in their mean arterial blood pressure to 87.5 mmHg, compared with 102 mmHg during AW (P = 0.012). The oxyhemoglobin saturation

‡‡‡ Available at: www.fil.ion.ucl.ac.uk/spm/software/spm5/. Accessed May 16, 2013.

§§§ Available at: www.icatb.sourceforge.net. Accessed May 16, 2013.

showed a small but statistically significant decline from 98 to 96% (P = 0.001), whereas the changes in heart rate, respiratory rate, and end-expiratory carbon dioxide were not significant (table 1, see Supplemental Digital Content 1, http://links.lww.com/ALN/A974, which is a table showing mean values of propofol plasma concentrations and cardiorespiratory monitoring parameters during AW and PI-LOC).

Effects of PI-LOC on Electroencephalographic PeEn and on STEn (DC)

From AW to PI-LOC, PeEn showed a significant decline of parameter values, as indicated by an AUC = 0.83 (0.55–1.00) at the frontal electrodes, whereas changes in parietal, temporal, and occipital were not significant (fig. 1, see Supplemental Digital Content 2, http://links.lww.com/ALN/A975, which is a figure indicating values of PeEn during AW and PI-LOC).

Symbolic transfer entropy $STEn_{X\to Y}$ and $STEn_{Y\to X}$ indicated a nonzero information transfer for both directions and for all electrode combinations during AW and PI-LOC (*i.e.*, $STEn_{X\to Y}, STEn_{Y\to X} > 0$ at $P < 0.05$).

Directionality index STEn showed a change of information direction from AW to PI-LOC in specific electrode combinations: A maximum decrease of STEn was found between frontal and parietal electrodes, as indicated by an AUC = 0.92 (0.68–1.00). This is related to a reverse of information transfer indicating a predominant unidirectional feedback flow at AW and a feedforward flow during PI-LOC (fig. 2 from article, and fig. 2, see Supplemental Digital Content 2, http://links.lww.com/ALN/A975, which is a figure indicating values of STEn, $STEn_{X\to Y}, STEn_{Y\to X}$ during AW and PI-LOC). Thereby, feedback (frontal to parietal) flow decreased from AW to PI-LOC (table 1).

During AW, the STEn showed a balanced bidirectional information exchange among the frontal and central electrodes, whereas the posterior parietal and occipital electrodes primarily received information (fig. 2A). In contrast, at PI-LOC the STEn showed a decreased bidirectional information exchange between the frontal and the posterior (parietal, temporal, and occipital) electrodes, resulting in a more unidirectional feedforward information flow (fig. 2B). This shift of information exchange was indicated by a decrease in top–down interaction ($STEn_{X\to Y}$) from the frontal to posterior electrodes, whereas the bottom–up interaction ($STEn_{Y\to X}$) was persevered during PI-LOC (table 1).

Validity of electroencephalographic analysis was demonstrated by the following results: First, no statistical differences were observed between STEn obtained from recordings outside the MRI scanner and during fMRI at AW. Second, STEn did not show statistical differences between both montages (average reference and FCz). Third, during AW and during PI-LOC, $STEn_{X\to Y}$ ($STEn_{Y\to X}$) from the electroencephalogram recording indicated higher values than $STEn_{X\to Y}$ ($STEn_{Y\to X}$) from surrogates in all considered electrode combinations ($P < 0.05$). In contrast to STEn obtained from the electroencephalogram recording, surrogate-based STEn failed to show effects of propofol in any electrode combinations.

Effects of PI-LOC on fMRI FC

The fMRI data of three subjects had to be excluded because of movement artifacts. We found preserved synchronized spontaneous BOLD fluctuations during PI-LOC. Higher-order frontoparietal networks (*i.e.*, posterior and anterior DMN, left and right frontoparietal attention networks) and lower-order sensory networks (*i.e.*, primary auditory cortex and primary visual cortex) could be consistently identified during both conditions. During PI-LOC, the intrinsic FC of the analyzed networks showed a dichotomous behavior. Although the FC within higher-order frontoparietal networks (*i.e.,* anterior and posterior DMN, left and right

Table 1. Changes of Electroencephalographic STEn under PI-LOC

Electrode Combinations X–Y	STEn AUC (CI) AW → PI-LOC	$STEn_{X\to Y}$ AUC (CI) AW → PI-LOC	$STEn_{Y\to X}$ AUC (CI) AW → PI-LOC
Frontal–parietal	↓ 0.92 (0.68–1.00)*	↓ 0.77 (0.59–0.93)	0.50 (0.27–0.72)
Frontal–temporal	↓ 0.61 (0.24–0.91)	↓ 0.52 (0.31–0.73)	↑ 0.41 (0.21–0.62)
Frontal–occipital	↓ 0.82 (0.53–1.00)*	↓ 0.79 (0.61–0.94)	↓ 0.56 (0.35–0.77)
Parietal–temporal	↓ 0.74 (0.40–0.97)	↓ 0.85 (0.69–0.98)	↓ 0.76 (0.58–0.91)
Parietal–occipital	↓ 0.55 (0.23–0.88)	↓ 0.75 (0.57–0.91)	↓ 0.73 (0.54–0.89)
Temporal–occipital	↓ 0.64 (0.24–0.94)	↓ 0.78 (0.60–0.93)	↓ 0.73 (0.53–0.89)

AUC and 95% percentile bootstrap CIs of STEn ($STEn_{X\to Y}$, $STEn_{Y\to X}$) and directionality index (STEn) from AW to PI-LOC. AUC >0.50 of STEn indicates a decrease (↓) of information exchange form X to Y, whereas AUC <0.50 of STEn indicates an increase (↑), respectively. AUC >0.50 of $STEn_{X\to Y}$ and $STEn_{Y\to X}$ indicates a decrease (↓) of unidirectional information flow between respective electrodes from AW to PI-LOC, AUC <0.50 an increase (↑), respectively. Only uncorrected 95% CI (threshold $P < 0.05$) without indication of significance were reported for $STEn_{X\to Y}$ and $STEn_{Y\to X}$ because both measures inherit information of STEn.

* 95% CI which exclude an AUC of 0.50 (random classifier) indicate significant changes of STEn (AW vs. PI-LOC, corrected threshold $P < < 0.05$ two-tailed).

AUC = area under receiver characteristic curve; AW = at wakefulness; CI = confidence interval; PI-LOC = propofol-induced loss of consciousness STEn = symbolic transfer entropy; X, Y = electroencephalographic electrode pair cluster consisting of cluster X and Y; ↓ = decrease of $STEn_{X\to Y}$, $STEn_{Y\to X}$, STEn; ↑ = increase of $STEn_{X\to Y}$, $STEn_{Y\to X}$, STEn.

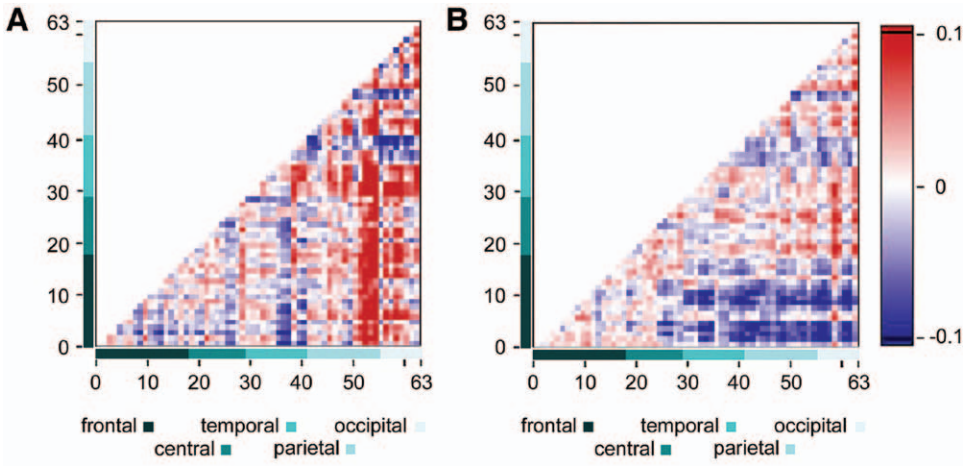

Fig. 2. Symbolic transfer entropy (STEn) directionality index at wakefulness (AW; *A*) and during propofol-induced loss of consciousness (PI-LOC; *B*). The maps show average values of STEn for each electrode combination in all 15 subjects: STEn >0 (color coded in *red*) indicates that electroencephalogram recordings from the electrodes on the vertical axis drives electroencephalogram recordings from electrodes on the horizontal axis; STEn <0 (color coded in *blue*) indicates that electroencephalogram recording from the electrodes on the vertical axis is driven by the electroencephalogram recording from electrodes on the horizontal axis. During AW, the STEn showed a balanced bidirectional information exchange among the frontal, central, and temporal electrodes, whereas the posterior parietal and occipital electrodes primarily received information (*A*). PI-LOC resulted in a significant decrease in feedback information flow from the frontal to the posterior temporal, parietal, and occipital electrodes (*B*).

frontoparietal attention networks) significantly decreased, the FC within primary sensory networks (*i.e.*, the primary auditory and visual cortices) significantly increased (table 2 and fig. 3). Of the DMN, the medial anterior prefrontal cortex, precuneus, and posterior cingulate cortex exhibited decreased FC (*i.e.*, were less integrated into the network). Furthermore, a significant uncoupling of the thalamus and cortical ICNs was observed (AW: partial-η^2 = 0.12; PI-LOC: partial-η^2 = 0.03; P = 0.0035; main effect of condition, df = 1; F = 15.44).

Table 2. Changes of fMRI FC under PI-LOC

Network	Cluster	Cluster Size (Number of Voxel)	MNI Coordinates of Peak Voxel (mm)			*z* Values (Peak Voxel)
			x	y	z	
Posterior DMN	Bilateral medial anterior prefrontal cortex (peak at mid orbital gyrus)	252	6	66	−10	−4.09
	Bilateral precuneus/posterior cingulate cortex	149	−4	−60	30	−3.95
Anterior DMN	Bilateral medial anterior prefrontal cortex (peak at mid orbital gyrus)	184	6	56	14	−4.31
Frontoparietal attention	Left lateral inferior prefrontal (peak at inferior frontal gyrus)	143	−50	38	−10	−4.05
	Right lateral inferior prefrontal (peak at inferior frontal gyrus)	164	50	44	−20	−4.39
	Right dorsolateral prefrontal (peak at superior frontal gyrus)	272	34	20	56	−4.36
Primary auditory	Right superior temporal lobe (peak at Heschl gyrus/superior temporal gyrus)	655	40	−22	6	+4.28
	Left superior temporal lobe (peak at Heschl gyrus/superior temporal gyrus)	203	−56	−16	6	+3.16*
Primary visual	Bilateral cuneus (peak at calcarine gyrus)	3,592	−16	−90	28	+5.40

fMRI FC, full-factorial ANOVA (n = 12): T-contrast of condition-specific effects, we report only cluster at a family-wise error corrected extent threshold P < 0.05 at an uncorrected voxel threshold P < 0.001.

* At the left primary auditory cortex, for which we had a specific hypothesis (*a priori*, and also by effects on the right side), we lowered the underlying voxel threshold to P < 0.005.

DMN = default mode network; FC = functional connectivity; fMRI = functional magnetic resonance imaging; MNI = Montreal Neurological Institute; PI-LOC = Propofol-induced loss of consciousness; x, y, z = MNI coordinates.

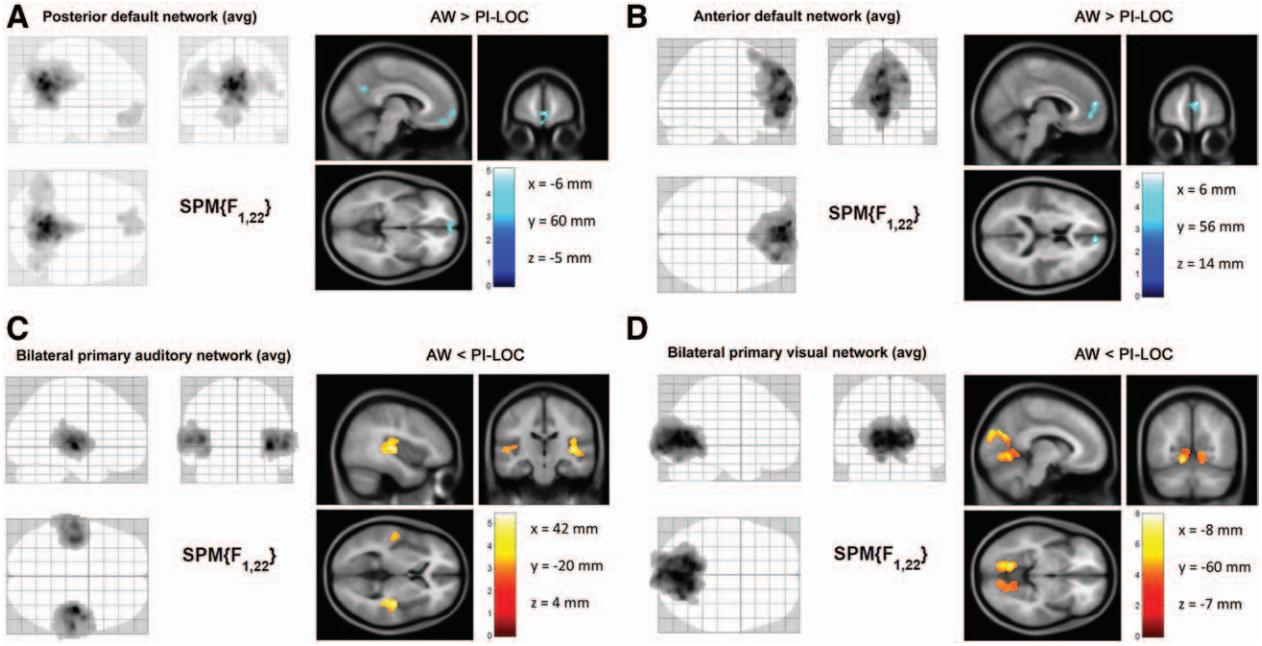

Fig. 3. Effects of propofol-induced loss of consciousness (PI-LOC) on functional magnetic resonance imaging functional connectivity (FC). The FC analysis of resting-state brain networks during PI-LOC showed decreased FC in the posterior (*A*) and anterior (*B*) default mode network, whereas the auditory (*C*) and visual (*D*) primary sensory networks showed increased FC. On the left, the average (avg) network for 12 subjects is displayed on the glass brain template of statistical parametric mapping (SPM) 8 (Wellcome Trust Centre for Neuroimaging, University of London, London, United Kingdom; full-factorial ANOVA, F-contrast over all subjects and conditions at the family-wise error-corrected cluster threshold $P < 0.05$ and the uncorrected voxel threshold $P < 0.001$) for both conditions (at wakefulness [AW]; PI-LOC). On the right, significant intrinsic FC changes between AW and PI-LOC are displayed on the average T1 brain template of SPM 8 (full-factorial ANOVA: T-contrast of condition-specific effects at the same thresholds, with the exception of the primary auditory cortex. Here, only the right auditory cortex survived a family-wise error-corrected cluster threshold at the predefined voxel threshold of $P < 0.001$; after lowering the (whole-brain) voxel threshold to $P < 0.005$, we also found significant family-wise error-corrected changes in FC in the left auditory cortex). The *red to yellow scales* indicate increased FC; the *dark to light blue scales* indicate decreased FC.

Correlation between FC and DC

The analysis was performed on the data of the 10 subjects for whom we had complete simultaneous electroencephalographic–fMRI data sets (in 2 of the 12 subjects included in the fMRI analysis, parts of the electroencephalogram were too noisy for a reliable analysis). Partial correlations were performed between fMRI FC of identified higher-order frontoparietal networks (*i.e.,* posterior and anterior DMN) and DC (STEn) in all electrode combinations. The propofol-induced decrease in FC of the anterior DMN within the individual was significantly correlated with the change of information direction (STEn) in following electroencephalographic electrode combinations (table 3): frontal → parietal ($r_{partial}$ = +0.62; P = 0.030) and frontal → occipital ($r_{partial}$ = +0.63; P = 0.048). All other correlations between FC of the DMN (posterior and anterior) and DC were not significant. Considering the results of fMRI FC (main effects of propofol within the frontoparietal DMN) and electroencephalographic DC (main effects within the frontal–posterior electrodes), Bonferroni correction was only applied for correlations between the DMN and frontal–posterior electrodes.

Discussion

In the current study, we simultaneously measured fMRI and high-resolution electroencephalogram measurements during PI-LOC in order to investigate the meaning of FC changes in fMRI for cortical information processing during unconsciousness. We found that the known decoupling between higher-order frontal processes and posterior sensory processes in fMRI was correlated with the breakdown of top–down DC between the same networks in the electroencephalogram.

Correlation of FC in fMRI and DC in the Electroencephalogram

The correlation of FC and DC in the same cohort of subjects examines the underlying mechanisms of anesthesia-induced unconsciousness. To investigate the relationship between FC in fMRI (*i.e.*, spatiotemporal coherence of spontaneous BOLD fluctuations) and DC in the electroencephalogram (*i.e.*, information exchange between corresponding electroencephalographic channels, measured by STEn), we performed a partial correlation analysis of FC and DC. We found that the decreased FC in the anterior DMN is mainly

Table 3. Partial Correlation Analysis between the Individual Mean *z* Scores of the DMNs (FC) and the Mean Electroencephalographic STEn (DC)

	Anterior DMN	Postrior DMN
STEn frontal → parietal	$r_{partial}$ = +0.62 (*P* = 0.030)*	$r_{partial}$ = +0.14 (*P* = 0.329)
STEn frontal → temporal	$r_{partial}$ = +0.44 (*P* = 0.168)	$r_{partial}$ = +0.19 (*P* = 0.956)
STEn frontal → occipital	$r_{partial}$ = +0.63 (*P* = 0.048)*	$r_{partial}$ = +0.07 (*P* = 0.550)
STEn parietal → temporal	$r_{partial}$ = +0.46 (*P* = 0.215)	$r_{partial}$ = +0.30 (*P* = 0.629)
STEn parietal → occipital	$r_{partial}$ = −0.15 (*P* = 0.936)	$r_{partial}$ = +0.04 (*P* = 0.853)
STEn temporal → occipital	$r_{partial}$ = +0.01 (*P* = 0.624)	$r_{partial}$ = −0.01 (*P* = 0.674)

Partial correlation analysis (coefficients $r_{partial}$) on the data of the 10 subjects for whom we had complete simultaneous electroencephalographic and functional fMRI data sets. Correlations were performed between fMRI FC of identified higher-order frontoparietal networks (*i.e.*, posterior and anterior DMN) and electroencephalographic DC of STEn directionality index (STEn) in all electrode combinations.

* Significant correlations at corrected threshold $P < 0.05$ (correction of *P* values includes only correlations between the DMN and three frontal → posterior STEns).

DC = directed connectivity; DMN = default mode network; FC = functional connectivity; fMRI = magnetic resonance imaging; $r_{partial}$ = correlation coefficient of partial correlation analysis; STEn = symbolic transfer entropy.

correlated with the decrease in top–down information flow from the frontal to the parietal and occipital electroencephalographic electrodes. This finding supports the significant role of frontal cortex interaction in conscious perception and demonstrates a direct correlation between the spatiotemporal coherence of spontaneous BOLD fluctuations in fMRI and information exchange between corresponding cortical areas in the electroencephalogram. This implies that the observed dichotomy between the FC of higher-order frontoparietal and the FC of posterior sensory networks reflects changes in cortical information processing. The observation of an impaired top–down access to sensory processes during general anesthesia is supported by an analysis of spectral electroencephalographic changes during PI-LOC. Dynamic causal modeling indicated that LOC was accompanied by a decrease in backward corticocortical connectivity from frontal to parietal cortices, whereas thalamocortical connectivity remained unchanged.[45]

On a more fundamental level, our observations are compatible with theories attributing consciousness to the capacity of the brain to integrate distributed information.[46] The observed decoupling of higher-order frontal and posterior sensory processes are reminiscent of Baars' "theater of consciousness metaphor,"[47] in which prefrontal areas act as a stage on which primary sensory information is displayed and spotlighted by attention processes. This is in accordance with results in previous graph theoretical analysis indicating a general reduction of whole-brain spatiotemporal integration with a pronounced breakdown of long-range corticocortical connections although no changes were found within primary sensory cortices.[11]

Effects of PI-LOC on FC in fMRI

In line with previous studies on anesthetized monkeys,[48] sedated,[8] anesthetized,[7,9,49] and sleeping[50–52] human subjects, as well as comatose patients,[53–55] we found preserved synchronized spontaneous BOLD fluctuations under PI-LOC. As hemodynamic and respiratory effects of propofol infusion may influence the fMRI data,[56] we monitored the respiratory rate and end-expiratory carbon dioxide levels but could not find any significant differences between AW and PI-LOC. Propofol administration resulted in decreased (mainly systolic) blood pressure, a known side effect of the drug.[57] This corresponds to positron emission tomography studies with propofol, which showed decreased cerebral blood flow[58] and raises the question of whether the observed effects in the fMRI resulted from FC changes or simply from changes in cerebral blood flow.

However, both our study, as well as previous studies[7] has shown different FC effects in different brain networks. This is strong evidence against a primary hemodynamic cause of the observed changes at the level of BOLD connectivity. Similar to Boveroux *et al.*[7] we found distinct effects of PI-LOC on higher-order frontoparietal networks and primary sensory networks. Although they found unchanged FC in primary sensory networks, the FC within these networks in our study actually increased. That these observations cannot be explained by pure pharmacological (hemodynamic) effects has been demonstrated by a previous positron emission tomography study that compared propofol and dexmedetomidin (an anesthetic drug that allows a return of consciousness without changing the plasma concentration) to differentiate the state-related changes from the pharmacological effects of the anesthetic drugs.[59] A combined analysis of both drugs revealed that the return of consciousness involved activation of the brainstem, thalamus, and the anterior cingulated cortex arousal networks that lead to a restored FC within the frontoparietal networks. We propose that both increased and decreased FC could be the result of thalamocortical and corticocortical decoupling. In distributed networks, such as the frontoparietal networks, thalamocortical decoupling may lead to disintegration of the network. In local networks, such as primary sensory networks, decoupling from the input (thalamus) and from the feedback by higher-order frontoparietal processes leads to a decoupling of the local processes and increased synchronization within

these local modules. Following this argumentation, it could be shown that increased FC in primary sensory cortices during unconsciousness reflects a kind of self-employment rather than functional relevant sensory processing.

Effects of PI-LOC on DC in the Electroencephalogram

Symbolic transfer entropy analysis of the electroencephalogram recordings revealed a change of directionality of information exchange between frontal and posterior (parietal and occipital) electrodes from AW to PI-LOC. Whereas the top–down flow was predominant at AW, a breakdown of top–down communication and prevailed bottom–up flow was observed at PI-LOC. The maintained unidirectional feedforward interaction in electroencephalographic DC along with a decreased FC in the frontoparietal DMN emphasizes a different meaning of connectivity: FC reflects the spatiotemporal coherence of hemodynamic fluctuations and may indicate the network's readiness to integrate information, whereas DC directly captures the actual interactions on a systemic processing level. Therefore, decreased FC is not necessarily related to a suppressed DC but may indicate a changing behavior of mutual interaction in the electroencephalogram, *e.g.*, decreased feedback information flow. Our observation of impaired top–down information flow in high-resolution electroencephalogram supports recent eight-channel (frontal–parietal, frontal–temporal, and bihemispheric) electroencephalographic results from surgical patients under general anesthesia with ketamine, propofol, and sevoflurane,[16,18] indicating that impaired frontal-to-parietal feedback may be a general neurophysiological correlate of impaired consciousness. In contrast to Ku *et al.*[16] and Lee *et al.*,[18] we performed a high-resolution, 63-channel electroencephalographic analysis revealing possible effects among all cortical regions without *a priori* assumptions.

Using surrogates of the electroencephalogram recordings, we could demonstrate that STEn indicates signal characteristics beyond linear randomness of the power spectrum. Therefore, spurious causality related to spectral changes did not account for our primary findings. Likewise, possible montage-specific effects were considered by analyzing STEn based on average reference and on FCz reference. No differences were found between both montages. Nevertheless, previous analyses during propofol anesthesia that were based on electroencephalographic Granger causality reported contradictory results,[29,30] that is, an increase of frontal to posterior connectivity in electroencephalogram.[30] Robust nonparametric PeEn and STEn as used in the current investigation may provide reliable results, even if different embedding parameters, transfer delays, and montages are used for analysis.[16] The observed decoupling of posterior sensory and higher frontal processes is further supported by results from an fMRI study of an auditory verbal memory task under propofol sedation, which showed impaired connectivity of the primary auditory cortex with frontal regions.[60]

Electroencephalographic Monitoring of Depth of Anesthesia

Permutation entropy has been introduced as a reliable electroencephalographic measure to separate responsiveness and unresponsiveness during anesthesia.[23,61] The observed decrease of PeEn at unconsciousness in frontal electroencephalogram is related to the decreased FC of the frontoparietal ICN. It may indicate a decrease of frontal information processing during PI-LOC and correspondence between electroencephalographic information processing and functional integration of higher-order frontal networks in fMRI. Furthermore, this study shows that STEn separates AW from PI-LOC by reflecting the correlation between a consciousness state and cortical information processing. These considerations are not only of theoretical interest but also of clinical relevance for monitoring the hypnotic component of anesthesia. Electroencephalographic depth of anesthesia monitoring has been suggested as a technique supplementing standard monitoring to prevent intraoperative awareness. However, a recent study suggested a limited value of a commercially available electroencephalographic monitor for detecting intraoperative awareness.[62] Mechanism-based approaches as introduced by STEn represent a step forward for future electroencephalographic monitors as they may specifically address processes of cortical dynamics. Validated by independent data sets, our study demonstrates the potential of entropy-based measures (PeEn and STEn) for quantifying unconsciousness during general anesthesia by indicating changes in frontal to posterior information processing.

Conclusion

In summary, our findings show for the first time that changes in FC in fMRI during unconsciousness correlate with simultaneous changes in DC in the electroencephalogram. This indicates that one underlying mechanism of functional decoupling of "higher-order" frontal and "lower-order" parietal processes during unconsciousness is the breakdown of directional feedback connectivity. To what extent our observations can be generalized with respect to other anesthetics requires further investigation. Ultimately, the "chicken or the egg problem" needs to be addressed, that is, whether the observed changes in information processing between cortical networks are the cause or the result of thalamocortical decoupling. With our data at hand, we cannot properly address the causality between thalamic and cortical effects of propofol-induced unconsciousness. However, both the observed dissociation of impaired feedback connectivity and preserved feedforward connectivity in electroencephalogram recordings as well as the preserved intrinsic FC in primary sensory networks in fMRI suggest a primary effect on cortical dynamics.

The authors thank the members of the Research Group on Brain Mechanisms of Consciousness and Anesthesia of the Departments of Anesthesiology, Neurology, and Neuroradiology, Technische Universität München, Munich, Germany, for their help.

References

1. Alkire MT, Hudetz AG, Tononi G: Consciousness and anesthesia. Science 2008; 322:876–80
2. Brown EN, Lydic R, Schiff ND: General anesthesia, sleep, and coma. N Engl J Med 2010; 363:2638–50
3. Franks NP: General anaesthesia: From molecular targets to neuronal pathways of sleep and arousal. Nat Rev Neurosci 2008; 9:370–86
4. Grasshoff C, Drexler B, Rudolph U, Antkowiak B: Anaesthetic drugs: Linking molecular actions to clinical effects. Curr Pharm Des 2006; 12:3665–79
5. Baars BJ, Ramsøy TZ, Laureys S: Brain, conscious experience and the observing self. Trends Neurosci 2003; 26:671–5
6. Brown EN, Purdon PL, Van Dort CJ: General anesthesia and altered states of arousal: A systems neuroscience analysis. Annu Rev Neurosci 2011; 34:601–28
7. Boveroux P, Vanhaudenhuyse A, Bruno MA, Noirhomme Q, Lauwick S, Luxen A, Degueldre C, Plenevaux A, Schnakers C, Phillips C, Brichant JF, Bonhomme V, Maquet P, Greicius MD, Laureys S, Boly M: Breakdown of within- and between-network resting state functional magnetic resonance imaging connectivity during propofol-induced loss of consciousness. Anesthesiology 2010; 113:1038–53
8. Greicius MD, Kiviniemi V, Tervonen O, Vainionpää V, Alahuhta S, Reiss AL, Menon V: Persistent default-mode network connectivity during light sedation. Hum Brain Mapp 2008; 29:839–47
9. Mhuircheartaigh RN, Rosenorn-Lanng D, Wise R, Jbabdi S, Rogers R, Tracey I: Cortical and subcortical connectivity changes during decreasing levels of consciousness in humans: A functional magnetic resonance imaging study using propofol. J Neurosci 2010; 30:9095–102
10. Tononi G: Information integration: Its relevance to brain function and consciousness. Arch Ital Biol 2010; 148:299–322
11. Schröter MS, Spoormaker VI, Schorer A, Wohlschläger A, Czisch M, Kochs EF, Zimmer C, Hemmer B, Schneider G, Jordan D, Ilg R: Spatiotemporal reconfiguration of large-scale brain functional networks during propofol-induced loss of consciousness. J Neurosci 2012; 32:12832–40
12. Boly M, Garrido MI, Gosseries O, Bruno MA, Boveroux P, Schnakers C, Massimini M, Litvak V, Laureys S, Friston K: Preserved feedforward but impaired top-down processes in the vegetative state. Science 2011; 332:858–62
13. King JR, Bekinschtein T, Dehaene S: Comment on "Preserved feedforward but impaired top-down processes in the vegetative state". Science 2011; 334:1203; author reply 1203
14. Imas OA, Ropella KM, Ward BD, Wood JD, Hudetz AG: Volatile anesthetics disrupt frontal-posterior recurrent information transfer at gamma frequencies in rat. Neurosci Lett 2005; 387:145–50
15. Jordan D, Ilg R, Wohlschläger A, Kochs EF, Schneider G: Information flow as electrophysiological signature of cortical connectivity during consciousness and propofol-induced unconsciousness. Br J Anaesth 2012; 108:334–67P, 44–5
16. Ku SW, Lee U, Noh GJ, Jun IG, Mashour GA: Preferential inhibition of frontal-to-parietal feedback connectivity is a neurophysiologic correlate of general anesthesia in surgical patients. PLoS One 2011; 6:e25155
17. Lee U, Kim S, Noh GJ, Choi BM, Hwang E, Mashour GA: The directionality and functional organization of frontoparietal connectivity during consciousness and anesthesia in humans. Conscious Cogn 2009; 18:1069–78
18. Lee U, Ku S, Noh G, Baek S, Choi B, Mashour GA: Disruption of frontal-parietal communication by ketamine, propofol, and sevoflurane. Anesthesiology 2013; 118:1264–75
19. Pryor KO, Mehta M, Blackstock-Bernstein AS, Feiler D, Veselis RA, Root JC: The conventional assumptions of blood-oxygen-level-dependent (BOLD) analysis of fMRI images are not altered by propofol: Evidence from three human subject study designs. Paper presented at: Annual Meeting of American Society of Anesthesiologists, Washington, D.C., October 15, 2012, A219
20. Friston KJ: Functional and effective connectivity: A review. Brain Connect 2011; 1:13–36
21. Staniek M, Lehnertz K: Symbolic transfer entropy. Phys Rev Lett 2008; 100:158101
22. Bandt C, Pompe B: Permutation entropy: A natural complexity measure for time series. Phys Rev Lett 2002; 88:174102
23. Jordan D, Stockmanns G, Kochs EF, Pilge S, Schneider G: Electroencephalographic order pattern analysis for the separation of consciousness and unconsciousness: An analysis of approximate entropy, permutation entropy, recurrence rate, and phase coupling of order recurrence plots. Anesthesiology 2008; 109:1014–22
24. Marsh B, White M, Morton N, Kenny GN: Pharmacokinetic model driven infusion of propofol in children. Br J Anaesth 1991; 67:41–8
25. Ramsay MA, Savege TM, Simpson BR, Goodwin R: Controlled sedation with alphaxalone-alphadolone. Br Med J 1974; 2:656–9
26. Allen PJ, Josephs O, Turner R: A method for removing imaging artifact from continuous EEG recorded during functional MRI. Neuroimage 2000; 12:230–9
27. Cao Y, Tung WW, Gao JB, Protopopescu VA, Hively LM: Detecting dynamical changes in time series using the permutation entropy. Phys Rev E Stat Nonlin Soft Matter Phys 2004; 70(4 Pt 2):046217
28. Roca-González J, Vallverdú-Ferrer M, Caminal-Magrans P, Martínez-González F, Roca-Dorda J, Álvarez-Gómez JA: Effects of propofol anesthesia on nonlinear properties of EEG: Time-lag and embedding dimension, 4th European Conference of the International Federation for Medical and Biological Engineering, Antwerp, Belgium, Springer-Verlag Berlin Heidelberg, 2008, pp 1268–71
29. Barrett AB, Murphy M, Bruno MA, Noirhomme Q, Boly M, Laureys S, Seth AK: Granger causality analysis of steady-state electroencephalographic signals during propofol-induced anaesthesia. PLoS One 2012; 7:e29072
30. Nicolaou N, Hourris S, Alexandrou P, Georgiou J: EEG-based automatic classification of 'awake' *versus* 'anesthetized' state in general anesthesia using Granger causality. PLoS One 2012; 7:e33869
31. Schreiber T: Measuring information transfer. Phys Rev Lett 2000; 85:461–4
32. Hipp JF, Engel AK, Siegel M: Oscillatory synchronization in large-scale cortical networks predicts perception. Neuron 2011; 69:387–96
33. Wang XJ: Neurophysiological and computational principles of cortical rhythms in cognition. Physiol Rev 2010; 90:1195–268
34. Davison AC, Hinkley DV: Bootstrap Methods and Their Application. Cambridge, Cambridge University Press, 1997
35. Jordan D, Steiner M, Kochs EF, Schneider G: A program for computing the prediction probability and the related receiver operating characteristic graph. Anesth Analg 2010; 111:1416–21
36. Luginbühl M, Schumacher PM, Vuilleumier P, Vereecke H, Heyse B, Bouillon TW, Struys MM: Noxious stimulation response index: A novel anesthetic state index based on hypnotic-opioid interaction. Anesthesiology 2010; 112:872–80
37. Karniski W, Blair RC, Snider AD: An exact statistical method for comparing topographic maps, with any number of subjects and electrodes. Brain Topogr 1994; 6:203–10
38. Schreiber T, Schnitz A: Surrogate time series. Physica D 2000; 142:346–82
39. Sorg C, Riedl V, Mühlau M, Calhoun VD, Eichele T, Läer L, Drzezga A, Förstl H, Kurz A, Zimmer C, Wohlschläger AM: Selective changes of resting-state networks in individuals at

risk for Alzheimer's disease. Proc Natl Acad Sci U S A 2007; 104:18760–5

40. Bell AJ, Sejnowski TJ: An information-maximization approach to blind separation and blind deconvolution. Neural Comput 1995; 7:1129–59
41. Himberg J, Hyvärinen A, Esposito F: Validating the independent components of neuroimaging time series *via* clustering and visualization. Neuroimage 2004; 22:1214–22
42. Damoiseaux JS, Rombouts SA, Barkhof F, Scheltens P, Stam CJ, Smith SM, Beckmann CF: Consistent resting-state networks across healthy subjects. Proc Natl Acad Sci U S A 2006; 103:13848–53
43. Bland JM, Altman DG: Calculating correlation coefficients with repeated observations: Part 1—Correlation within subjects. BMJ 1995; 310:446
44. Bland JM, Altman DG: Agreement between methods of measurement with multiple observations per individual. J Biopharm Stat 2007; 17:571–82
45. Boly M, Moran R, Murphy M, Boveroux P, Bruno MA, Noirhomme Q, Ledoux D, Bonhomme V, Brichant JF, Tononi G, Laureys S, Friston K: Connectivity changes underlying spectral EEG changes during propofol-induced loss of consciousness. J Neurosci 2012; 32:7082–90
46. Tononi G, Koch C: The neural correlates of consciousness: An update. Ann N Y Acad Sci 2008; 1124:239–61
47. Baars BJ: Global workspace theory of consciousness: Toward a cognitive neuroscience of human experience. Prog Brain Res 2005; 150:45–53
48. Vincent JL, Patel GH, Fox MD, Snyder AZ, Baker JT, Van Essen DC, Zempel JM, Snyder LH, Corbetta M, Raichle ME: Intrinsic functional architecture in the anaesthetized monkey brain. Nature 2007; 447:83–6
49. Stamatakis EA, Adapa RM, Absalom AR, Menon DK: Changes in resting neural connectivity during propofol sedation. PLoS One 2010; 5:e14224
50. Horovitz SG, Braun AR, Carr WS, Picchioni D, Balkin TJ, Fukunaga M, Duyn JH: Decoupling of the brain's default mode network during deep sleep. Proc Natl Acad Sci U S A 2009; 106:11376–81
51. Larson-Prior LJ, Zempel JM, Nolan TS, Prior FW, Snyder AZ, Raichle ME: Cortical network functional connectivity in the descent to sleep. Proc Natl Acad Sci U S A 2009; 106: 4489–94
52. Spoormaker VI, Schröter MS, Gleiser PM, Andrade KC, Dresler M, Wehrle R, Sämann PG, Czisch M: Development of a large-scale functional brain network during human non-rapid eye movement sleep. J Neurosci 2010; 30:11379–87
53. Boly M, Phillips C, Tshibanda L, Vanhaudenhuyse A, Schabus M, Dang-Vu TT, Moonen G, Hustinx R, Maquet P, Laureys S: Intrinsic brain activity in altered states of consciousness: How conscious is the default mode of brain function? Ann N Y Acad Sci 2008; 1129:119–29
54. Boly M, Tshibanda L, Vanhaudenhuyse A, Noirhomme Q, Schnakers C, Ledoux D, Boveroux P, Garweg C, Lambermont B, Phillips C, Luxen A, Moonen G, Bassetti C, Maquet P, Laureys S: Functional connectivity in the default network during resting state is preserved in a vegetative but not in a brain dead patient. Hum Brain Mapp 2009; 30:2393–400
55. Crone JS, Ladurner G, Höller Y, Golaszewski S, Trinka E, Kronbichler M: Deactivation of the default mode network as a marker of impaired consciousness: An fMRI study. PLoS One 2011; 6:e26373
56. Chang C, Cunningham JP, Glover GH: Influence of heart rate on the BOLD signal: The cardiac response function. Neuroimage 2009; 44:857–69
57. Plourde G, Belin P, Chartrand D, Fiset P, Backman SB, Xie G, Zatorre RJ: Cortical processing of complex auditory stimuli during alterations of consciousness with the general anesthetic propofol. Anesthesiology 2006; 104:448–57
58. Kaisti KK, Metsähonkala L, Teräs M, Oikonen V, Aalto S, Jääskeläinen S, Hinkka S, Scheinin H: Effects of surgical levels of propofol and sevoflurane anesthesia on cerebral blood flow in healthy subjects studied with positron emission tomography. Anesthesiology 2002; 96:1358–70
59. Långsjö JW, Alkire MT, Kaskinoro K, Hayama H, Maksimow A, Kaisti KK, Aalto S, Aantaa R, Jääskeläinen SK, Revonsuo A, Scheinin H: Returning from oblivion: Imaging the neural core of consciousness. J Neurosci 2012; 32:4935–43
60. Liu X, Lauer KK, Ward BD, Rao SM, Li SJ, Hudetz AG: Propofol disrupts functional interactions between sensory and high-order processing of auditory verbal memory. Hum Brain Mapp 2012; 33:2487–98
61. Olofsen E, Sleigh JW, Dahan A: Permutation entropy of the electroencephalogram: A measure of anaesthetic drug effect. Br J Anaesth 2008; 101:810–21
62. Avidan MS, Jacobsohn E, Glick D, Burnside BA, Zhang L, Villafranca A, Karl L, Kamal S, Torres B, O'Connor M, Evers AS, Gradwohl S, Lin N, Palanca BJ, Mashour GA; BAG-RECALL Research Group: Prevention of intraoperative awareness in a high-risk surgical population. N Engl J Med 2011; 365:591–600